Inhibition of growth in solid solution–aqueous solution systems by non-incorporating impurities

Carlos M. Pina

Department of Crystallography and Mineralogy, Complutense University of Madrid, c/ José Antonio Novais 2, Madrid E-28040, Spain

Keywords:
Crystal growth inhibition
Impurities
Solid solution–aqueous solution systems

A B S T R A C T

Crystal growth inhibition by non-incorporating impurities has been described and quantified since 1958 by the so-called step pinning model by Cabrera and Vermilyea [1]. In the original model, as well as in its recent improvements by Weaver et al. in 2006 and 2007 [2,3], only the inhibition by the adsorption of impurities on crystal surfaces with fixed compositions is considered. However, most of the crystals found in nature are solid solutions with more or less wide chemical variability. Therefore, in order to provide more realistic models of crystal growth inhibition in natural systems, it is fundamental to study in detail the inhibition of surfaces of solid solutions by non-incorporating impurities. In this paper, the Cabrera–Vermilyea model has been generalised for the case of growth inhibition in solid solution–aqueous solution (SS–AS) systems. This generalisation was made by considering that supersaturation and the physicochemical properties of the solid solutions are functions of the solid composition. The main implication of the model is that a progressive inhibition of growth of a solid solution by increasing the concentration of an adsorbed impurity results in compositional changes on the growing surfaces.

1. Introduction

Inhibition of crystal growth by impurities plays a fundamental role in the crystallisation processes taking place both in nature and industry. Usually, only very low concentrations of these impurities are enough to partially or completely inhibit growth on crystal faces. This fact has been recognised by living organisms, which have been using for millions of years a wide variety of molecules as inhibitors to avoid pathological mineralization from bodily fluids (e.g. kidney and gall bladder stones, and mineralization within soft tissues such as veins or digestive tracts [2,3]). Furthermore, organisms can also use molecules in a more sophisticated way to modify and control the crystal growth behaviour of common minerals (e.g. calcite, aragonite, apatite). In doing so, they are able to construct complex biological structures with specific forms and physical properties (e.g. endo and exoskeletons, navigation systems in bacteria, and gravity sensors in mammals [4]).

But not only organisms take advantage of inhibitors of crystal growth. Many industrial activities also require the usage of chemical compounds that inhibit mineral formation. For instance, phosphonates have been used to prevent undesirable barite mineralization in marine oil and gas wells where the concentrations of sulphate and barium ions are high [5–7]. In a similar vein, phosphate-based inhibitors and phosphonates have been employed to avoid calcite formation in pipes, cooling and boiling water systems, and desalination facilities in regions with highly carbonated waters [8,9]. In these and in other many cases in which the prevention of mineralization is required, it is fundamental to find the most adequate inhibitors and to optimize their concentrations.

Therefore, in order to understand, predict and control biomineralization and mineralization in a number of industrial processes, a profound knowledge of the mechanisms governing the inhibition of crystal growth is necessary. Proposed physical models conceive crystal growth inhibition as the result of a progressive poisoning of the growth sites on crystal surfaces by impurities. When these impurities are large molecules that cannot incorporate into the crystal structure, inhibition is considered to occur by the adsorption of such molecules on the crystal surfaces and the subsequent pinning of the growing steps. By increasing the concentration of impurities, the step pinning becomes more severe and finally steps cannot propagate over the crystal surface. Then, the complete inhibition of growth occurs.

In the original Cabrera–Vermilyea model of step pinning, as well as in a recent reformulation of it [1–3], the progressive decrease in step velocity as a consequence of the increase in the concentration of impurities is analysed in terms of both the degree of coverage of the crystal surface by the adsorbed impurities and the free energy of steps with different curvatures (i.e. the Gibbs–Thomson effect). This analysis assumes a fixed composition of the crystal. However, crystallisation in natural aqueous systems leads, almost without exceptions, to the formation of solid solutions with more or less wide compositional ranges. Since the chemical variability of a crystal implies variability in its surface properties, the development of more

E-mail address: cmpina@geo.ucm.es.

realistic models of crystal growth inhibition in natural aqueous environments requires an analysis of the effect of the composition on the inhibition mechanism.

The aim of this paper is to reformulate the Cabrera–Vermilyea model of step pinning for the case of the inhibition of solid solutions by non-incorporating impurities. To this end, concepts from the theory of solid solution–aqueous solution (SS–AS) systems [10,11] have been incorporated into the classical equations for the critical radius, the critical supersaturation, the Gibbs–Thomson effect, and the step velocity. Although the reformulation can be applied to any solid solution with general formula $B_xC_{1-x}A$, the physicochemical parameters of barite–celestite ($Ba_xSr_{1-x}SO_4$) solid solution have been used to illustrate the main implications of the generalised Cabrera–Vermilyea model. In the last two decades, the thermodynamical properties of barite and celestite crystals, as well as their interactions with inorganic and organic impurities, have been studied extensively (e.g. [6,7,12–18]). In addition, atomic force microscopy studies have provided detailed information about the nano-scale growth mechanisms operating on barite and celestite surfaces (e.g. [6,7,10,19]). Therefore, the $Ba_xSr_{1-x}SO_4$ solid solution represents a suitable model example for both illustrative purposes and future experimental testing of the model presented in this paper.

2. Theoretical background

2.1. Supersaturation in solid solution aqueous solution (SS–AS) systems

Supersaturation is the reference parameter in any study of inhibition of crystal growth by inorganic or organic impurities. Both growth inhibition mechanisms and inhibition effectiveness are determined by the modification of the step kinetics at different supersaturations and inhibitor concentrations. In the case of binary ionic solids with the general formula *AB*, supersaturation is frequently expressed by:

$$\beta = \frac{a(B^+)\,a(A^-)}{K_{sp}} = e^{\sigma} \tag{1}$$

where $a(B^+)$ and $a(A^-)$ are the activities of the constituting ions of the solid in the aqueous solution, K_{sp} is the solubility product of the solid phase and σ is the so-called thermodynamic supersaturation [12,20]. Eq. (1) can be generalised for the case of binary solid solutions with the general formula $B_xC_{1-x}A$. This generalisation leads to the definition of the so-called stoichiometric supersaturation function [11,21,22]:

$$\beta(x) = \frac{a(B^+)^x a(C^+)^{1-x} a(A^-)}{(K_{BA}X_{BA}\xi_{BA})^x (K_{CA}X_{CA}\xi_{CA})^{1-x}} \tag{2}$$

where $a(A^-)$, $a(B^+)$ and $a(C^+)$ are the activities of the ions in the aqueous solution; K_{BA} and K_{CA} are the solubility products of the end-members of the solid solution; X_{BA} and X_{CA} are the mole fractions of *BA* and *CA* components in the solid solution; ξ_{BA} and ξ_{CA} are the activity coefficients of *BA* and *CA* in the solid ($\xi_{BA}=\xi_{CA}=1$ for the case of an ideal solid solution) and x is the stoichiometric number which varies from 0 to 1. Eq. (2) means that, for an aqueous solution with given concentrations of the A^-, B^+ and C^+ ions, each solid solution composition has a value of supersaturation (see Fig. 1).

2.2. The Cabrera–Vermilyea model of growth inhibition

In the Cabrera–Vermilyea model, the inhibition of growth on a crystal surface is considered to occur by means of the pinning of monomolecular steps by impurities (see Fig. 2). Such impurities adsorb on the crystal terraces but they do not incorporate into the crystal structure, i.e. they do not form a solid solution. When the number of adsorbed impurities on the surface is low, curved segments of monosteps can propagate between the positions where such steps are pinned. By increasing the concentration of impurities on the surface, the advancement of steps between the adsorbed impurities becomes more difficult and step propagation is progressively reduced.

The complete inhibition of step motion on a crystal surface occurs when the average distance between adsorbed impurities, d_i, is less than twice the radius of the two-dimensional critical nucleus, ρ_c, i.e. when the step free energy of a curved step segment is higher than the reduction of chemical potential due to the incorporation of a growth unit from the aqueous solution into the step. The condition for inhibition $d_i<2\rho_c$ is, therefore, a direct consequence of the so-called Gibbs–Thomson effect, which relates the free energy of a monostep in contact with an aqueous solution with the curvature of such a step.

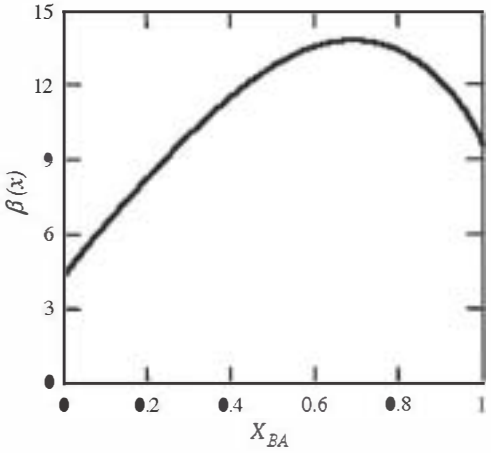

Fig. 1. Supersaturation function, $\beta(x)$, calculated for an aqueous solution of composition $a(A^-)=10^{-3}$, $a(B^+)=10^{-6}$, and $a(C^+)=10^{-3}$. The X_{BA} mole fraction is represented in abscissa. This supersaturation function has been calculated using Eq. (2) assuming an ideal $B_xC_{1-x}A$ solid solution ($\xi_{BA}=\xi_{CA}=1$) and with the following solubility products for the endmembers: $K_{BA}=10^{-9.98}$ and $K_{CA}=10^{-6.63}$.

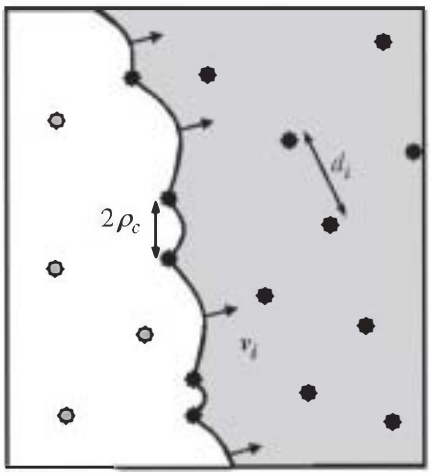

Fig. 2. Representation of a crystal surface on which impurities have pinned a monostep that separates two terraces (white: high terrace; grey: low terrace). According to the Cabrera–Vermilyea model, step segments can only grow between impurities when the distance between such impurities, d_i, is larger than twice the radius of the two-dimensional critical nucleus, ρ_c, i.e. the radius of the curved step. Since the ρ_c is related to the supersaturation by the Gibbs–Thomson effect, the advancement of a given step segment requires overcoming a critical supersaturation. Above the critical supersaturation, the step velocity, v_i, is given by Eq. (6). (See explanation in the text).

According to the classical theory of crystal growth, the dependence of the critical radius of a two-dimensional nucleus (i.e. the radius of a curved step) on the supersaturation is given by [23,24]:

$$\rho_c = \frac{\alpha\Omega}{kT\ln\beta} \tag{3}$$

where α is the crystal-solution interfacial free energy, Ω is the molecular volume of the growth unit, k is the Boltzmann constant and T is the absolute temperature.

Assuming that the degree of coverage of the surface by the impurity is proportional to its concentration in the aqueous solution, $[I]$, the following expression for the distance between impurities adsorbed on a crystal surface has been proposed [1–3]:

$$d_i = A\left(\frac{1}{[I]}\right)^{0.5} \tag{4}$$

where A is a proportionality constant. Considering the maximum distance between adsorbed impurities $d_i = 2\rho_c$, the combination of Eq. (3) and Eq. (4) yields the following expression of the critical supersaturation for complete growth inhibition:

$$\beta_c = e^{\frac{2\alpha\Omega B[I]^{0.5}}{kT}} \tag{5}$$

where B is a factor which combines the proportionality constant A with a number of parameters that quantify the adsorption behaviour of the impurity on the crystal surface, e.g. sticking probability, statistical variations in the impurity spacing, and the lifetime of the impurity on the surface [2,3]. Therefore, the B factor quantifies the effectiveness of adsorbed impurities for pinning the steps and it is especially relevant when reversible adsorption of impurities and dynamic equilibrium are considered.

For a given impurity concentration, Eq. (5) provides the minimum supersaturation required for observing step motion on a crystal surface. However, at supersaturations slightly higher than the critical supersaturation, some segments of a single step remain pinned and they propagate at lower velocities than the unpinned segments. According to the Cabrera–Vermilyea model, the overall velocity of a step above the critical supersaturation is the geometrical average of the velocities of pinned and unpinned segments of such a step:

$$v_i = \left[v_0\left(v_0 - \frac{v_0 \ln\beta_c}{\ln\beta}\right)\right]^{0.5} = v_0\left(1 - \frac{\ln\beta_c}{\ln\beta}\right)^{0.5} \quad \text{for } \ln\beta \geq \ln\beta_c \tag{6}$$

where v_0 is the velocity of the unpinned step segments, i.e. the velocity of a straight step segment. According to Eq. (6), by increasing supersaturation above the critical supersaturation for complete inhibition, the step velocity progressively increases until its characteristic linear dependency on the supersaturation of the pure system (i.e. in the absence of impurity) is reached [1,12,25].

3. Inhibition of growth on surfaces of solid solutions by non-incorporating impurities

The Cabrera–Vermilyea model for crystal growth inhibition summarised in the previous section assumes that the growing crystal has a fixed composition. However, this model can also be applied to the case of the growth inhibition by adsorbed impurities on crystal surfaces with variable composition (i.e. crystal surfaces of solid solutions). For this purpose it is, however, necessary to take into account that in SS–AS systems, supersaturation and the physico-chemical properties of solid solutions are functions of the solid composition. In the following sections, the consequences of the variability in the solid composition on the inhibition of crystal growth will be analysed in detail. As a result of the analysis, a generalised Cabrera–Vermilyea model for crystal growth inhibition in SS–AS systems is proposed.

3.1. Critical radius and critical supersaturation

In SS–AS systems, the critical radius of two-dimensional nucleus on a solid solution surface is not a single value but a function of the solid composition, which can be obtained by extending Eq. (3) to the whole range of solid solution compositions:

$$\rho_c(x) = \frac{\alpha(x)\Omega(x)}{kT\ln\beta(x)} \tag{7}$$

where $\beta(x)$ is the supersaturation function (Eq. (1)) and $\alpha(x)$ and $\Omega(x)$ are, respectively, the variation of the interfacial free energy and the variation of molecular volume of the growth unit from one endmember of the solid solution to the other (which as a first approximation can be considered as linear functions of the solid solution composition [10,12]). Fig. 3a shows the variation of the critical radius of the two-dimensional nucleus as a function of the composition of the solid, calculated for a solid solution with the supersaturation function shown in Fig. 1. As can be seen in Fig. 3a, each solid solution composition has a different value of the critical radius of the two-dimensional nucleus. This implies that, on a solid solution crystal surface with a given concentration of adsorbed impurities, only the solid solution compositions for which the $2\rho_c(x)$ function is smaller than d_i can squeeze between the impurities that pin the monosteps. As a consequence, the presence of pinning impurities on a solid solution surface in contact with a supersaturated aqueous solution can result in a chemical partitioning, where the compositions of the growing monosteps are determined by the concentration of adsorbed impurities. This effect is illustrated in the example of Fig. 3. In Fig. 3a the line $\rho_c = ½\ d_i = 0.6$nm has been drawn. The intersection of this line with the $\rho_c(x)$ curve gives the range of compositions of the monosteps that can grow between adsorbed impurities with a spacing of 1.2 nm. In this particular case, only steps with compositions $0.33 < X_{BA} < 0.63$ can advance on the crystal surface (see Fig. 3b).

Obviously, different combinations of supersaturation functions and concentrations of adsorbed impurities will result in different compositions of the growing steps. Therefore, the inhibition of growth on a given surface of a solid solution by increasing the impurity concentration leads to compositional changes in the surface until complete inhibition occurs. This compositional evolution of the surface will be determined by the initial supersaturation state of the solid solution as defined by the supersaturation function. At any stage of the growth process, only the solid solution compositions whose supersaturations are higher than their critical supersaturations grow. In SS–AS systems, the critical supersaturation for complete inhibition by adsorbed impurities is also a function of the solid solution composition:

$$\beta_c(x) = e^{\frac{2\alpha(x)\Omega(x)B[I]^{0.5}}{kT}} \tag{8}$$

In order to derive Eq. (8) it is assumed, as in the case of Eq. (5), that the degree of coverage of the surface by the impurity is proportional to its concentration in the aqueous solution (Eq. (4)). However, it has been recently pointed out that this assumption is not realistic in most crystal-aqueous solution systems. According to Kubota [26] and Weaver et al. [2,3], the degree of coverage of a crystal surface by a monolayer of impurities with a given concentration in the aqueous solution is better described by the Langmuir model of adsorption dynamics. The Langmuir mechanism

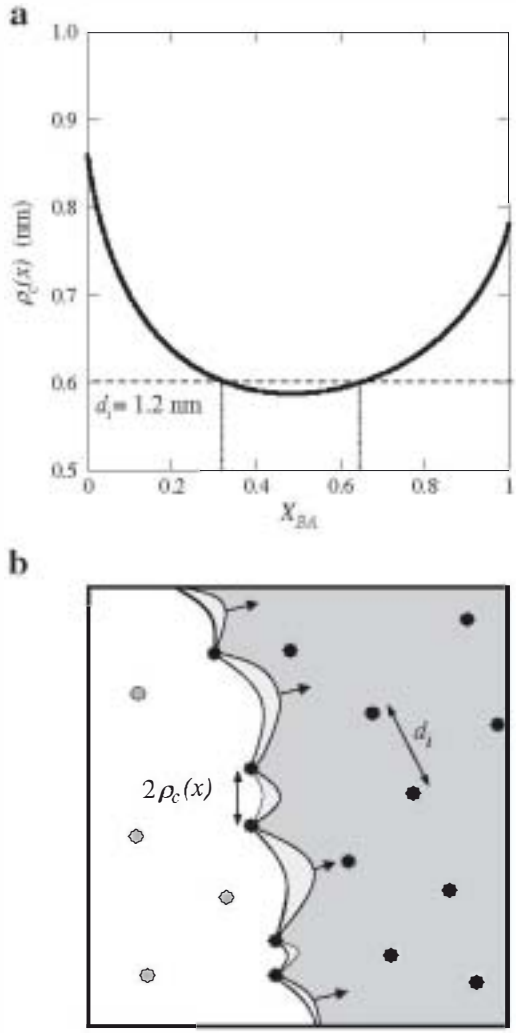

Fig. 3. (a) Variation of the critical radius of two-dimensional nuclei, $\rho_c(x)$, calculated for a solid solution with the supersaturation function shown in Fig. 1. The calculation was made using Eq. (7) and assuming a linear variation for both the interfacial free energy and the molecular volume of the growth unit. (Interfacial free energies for the solid solution endmembers: $\alpha_{BA}=84$ mJ/m^2; $\alpha_{CA}=67$ mJ/m^2; molecular volume of the endmembers: $\Omega_{BA}=8.64\times10^{-2}$ nm^3; $\Omega_{CA}=7.69\times10^{-2}$ nm^3). On this graph the horizontal dashed line $d_i=1.2$ nm has been drawn. This line gives the condition for the inhibition of step growth (see explanation in the text). (b) Representation of a surface of a solid solution crystal on which impurities have pinned a monostep. Only solid solution compositions for which $2\rho(x)<d_i$ can grow between the adsorbed impurities (represented in light grey).

of adsorption assumes a dynamic equilibrium involving the concentration of surface positions where the impurity can be adsorbed, the concentration of impurities in the aqueous solution, and the concentration of adsorbed impurities. From this assumption and by applying the mass law, the following equation for the so-called adsorption isotherm can be derived:

$$\theta_i = \frac{\left(k_A/k_D\right)[I]}{1+\left(k_A/k_D\right)[I]} \tag{9}$$

where θ_i is the fraction of the surface positions where the impurities are attached, and k_A and k_D are the impurity attachment and detachment rate coefficients, respectively. We will consider now that the distance between adsorbed impurities on the crystal surface is given by:

$$d_i = A\left(\frac{1}{\delta_i}\right)^{0.5} \tag{10}$$

with δ_i being the density of impurities adsorbed on the surface, which is:

$$\delta_i = \left(\frac{h}{\Omega}\right)\theta_i \tag{11}$$

where h is the height of the monostep. Combining Eq. (10) and Eq. (11) we obtain:

$$d_i = A\left(\frac{\Omega}{h\theta_i}\right)^{0.5} \tag{12}$$

Considering again the condition $d_i=2\rho_c$, and taking into account that h also varies linearly with the composition of the solid solution, the combination of Eq. (7), Eq. (12), and Eq. (9) gives the following expression for the critical supersaturation for inhibition based on the Langmuir adsorption model:

$$\beta_c(x) = e^{\left(B\frac{2\alpha(x)}{kT}(h(x)\Omega(x))^{0.5}\left[\frac{\left(k_A/k_D\right)[I]}{1+\left(k_A/k_D\right)[I]}\right]^{0.5}\right)} \tag{13}$$

Fig. 4a shows five critical supersaturation functions corresponding to our solid solution and calculated for five increasing concentrations of an inhibiting impurity. On the graph, the supersaturation function shown in Fig. 1 has been superimposed. Fig. 4a clearly shows that for each critical supersaturation function only steps with compositions with supersaturations higher than the critical supersaturation can advance over the crystal surface.

3.2. Step velocity

A key issue in the Cabrera–Vermilyea model is the quantification of the step velocity at supersaturations above the critical supersaturation. Such a quantification is based on the analysis of the dependence of the step velocity on the step curvature. Therefore, for the generalisation of the step kinetic equations of Cabrera and Vermilyea for SS–AS systems it is necessary to derive first the rate equations of curved and straight steps of a solid solution crystal. According to the surface diffusion theory of crystal growth [23,24], the derivation of rate equations for single steps requires: (i) to physically model the diffusion of growth units adsorbed on a crystal surface and (ii) to evaluate the supersaturation in the proximity of the growing steps. Taking this into account, Ohara and Reid proposed the following general rate equations for curved and straight steps, respectively [24]:

$$v_\rho = \frac{\Omega}{h}\left(\frac{2D_S C_{SE}}{X_S}\right)\left(S-S_\rho\right) \tag{14a}$$

$$v_\infty = \frac{\Omega}{h}\left(\frac{2D_S C_{SE}}{X_S}\right)(S-S_\infty) \tag{14b}$$

where v_ρ is the velocity of a curved step, v_∞ is the velocity of a straight step, D_S is the diffusion coefficient of the solute units on the crystal surface, C_{SE} is the equilibrium surface concentration of the solute units, X_S is the mean diffusion length of the solute units on a surface, S

is the supersaturation in the bulk, S_ρ is supersaturation in the proximity of a curved step, and S_0 is the supersaturation in the proximity of a straight step. Dividing Eq. (14a) by Eq. (14b) gives:

$$v_\rho = v_0 \frac{(S - S_\rho)}{(S - S_0)} \tag{15}$$

For a straight step there are no energy terms due to curvature and the step is assumed to be in equilibrium with the surrounding aqueous solution. Therefore, the supersaturation at the edge of a straight step is equal to the supersaturation in the bulk, i.e. $S_0 = 0$. Taking this into account, Eq. (15) becomes:

$$v_\rho = v_0 \left(1 - \frac{S_\rho}{S}\right) \tag{16}$$

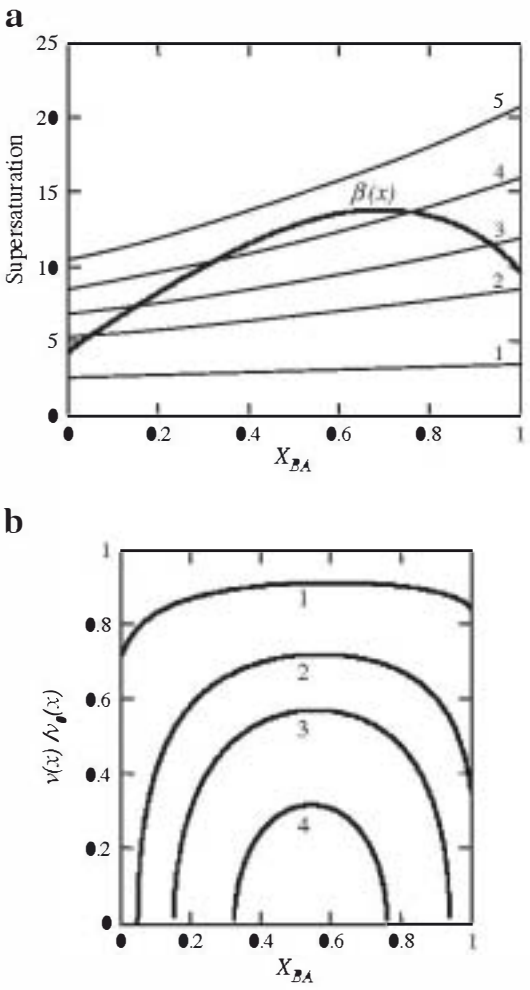

Fig. 4. (a) Five critical supersaturation functions calculated using Eq. (13) for a solid solution with the same physicochemical parameters and supersaturation state as those used to construct previous figures. The curves have been calculated for five aqueous solutions with increasing concentrations of the inhibiting impurity. (solution 1: $[I] = 0.5\,\mu M$; solution 2: $[I] = 1.5\,\mu M$; solution 3: $[I] = 2.0\,\mu M$; solution 4: $[I] = 2.5\,\mu M$; solution 5: $[I] = 3.0\,\mu M$) and using the following parameters: $B = 2.5 \times 10^3$; $k_A = 10^{-6}$; $k_0 = 10^{-4}$ and $h(x)$ varying linearly from 0.34 nm to 0.36 nm. On the graph, the supersaturation function shown in Fig. 1 is also drawn. Note that the range of compositions of the steps that can grow decreases from solution 1 to solution 4. For solution 5 the supersaturation function, $\beta(x)$, lies below the critical supersaturation curve and step growth is not possible. (b) Dependence of $v_i(x)/v_0(x)$ on the solid solution composition for the same concentrations of the inhibiting impurity used in (a). The curves have been calculated using Eq. (20).

Recognising the supersaturation equivalence [12,24] $S = \beta - 1$, Eq. (16) can be rewritten as:

$$v_\rho = v_0 \left(1 - \frac{\beta_\rho - 1}{\beta - 1}\right) \tag{17}$$

If we impose now the condition for complete inhibition of step motion on Eq. (17): $\beta_\rho = \beta_c$, the following rate equation for a pinned step by adsorbed impurities is obtained:

$$v_{pn} = v_0 \left(1 - \frac{\beta_c - 1}{\beta - 1}\right) \tag{18}$$

This equation is equivalent to that derived by Weaver et al. [3] from the expression of the Gibbs–Thomson effect, which is valid for all supersaturations [20].

As mentioned before, in the analysis by Cabrera and Vermilyea, the step velocity at supersaturations above the critical supersaturation is assumed to be the geometrical average of pinned and unpinned segment steps (Eq. (6)). From this assumption and using Eq. (18) for the velocity of the pinned steps, the velocity of the steps on a crystal surface with adsorbed impurities is given by:

$$v_i = v_0 \left(1 - \frac{\beta_c - 1}{\beta - 1}\right)^{0.5} \tag{19}$$

It is interesting to note that, taking into account the equivalence between supersaturations given by Eq. (1), Eq. (19) reduces to Eq. (6) at low supersaturations when the approximation $e^x = 1 + x$ can be used. When Eq. (19) is expressed for a SS–AS system it becomes:

$$v_i(x) = v_0(x) \left(1 - \frac{\beta_c(x) - 1}{\beta(x) - 1}\right)^{0.5} \text{ for } \beta(x) \geq \beta_c(x) \tag{20}$$

This equation describes the kinetics of growth of solid solution steps as a function of their composition and the inhibitor concentration. As an example, Fig. 4b shows the step velocities as a function of the solid composition for the same solid solution supersaturation function and inhibitor concentrations used to construct Fig. 4a. As can be seen in Fig. 4b, an increase in the inhibitor concentration not only leads to a decrease in step velocities but also results in a progressive reduction in the compositional range of the growing solid solution. This behaviour is better visualised in the three-dimensional graph shown in Fig. 5.

Graphs like that shown in Fig. 5 completely describe the changes in both growth rate and composition of solid solution steps when the concentration of a non-incorporating impurity is progressively increased. It is clear that different initial supersaturation states of an aqueous solution with respect to a solid solution will result in different kinetic and compositional paths toward the complete inhibition of growth. This suggests that some reported phenomena, such as anomalous growth rates observed during the inhibition of crystallisation in some chemically complex systems ([27] and references therein) and the development of heterogeneous element distributions onto mineral surfaces [28,29], might be related to the behaviour of crystal growth inhibition in SS–AS systems.

4. Conclusions and future work

In natural aqueous systems, inhibition of crystal growth by adsorbed impurities frequently occurs on mineral surfaces with variable composition, i.e. on solid solutions. Therefore, a better understanding and control of phenomena such as biomineralization, pathological mineralization in bodily fluids, undesirable mineral precipitation in pipes and oil wells, etc. requires models of crystal growth inhibition that incorporate the chemical variability of

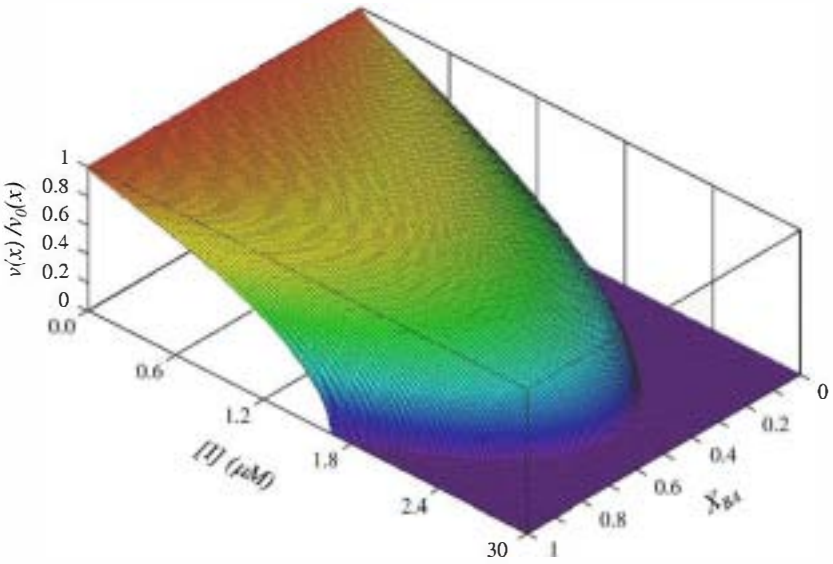

Fig. 5. Three-dimensional graph showing the dependence of $v_i(x)/v_0(x)$ on the solid solution composition and inhibitor concentration. The surface has been calculated using Eq. (20) for a SS–AS system with the same physicochemical and kinetic parameters, and for a critical supersaturation function (Eq. 13) and supersaturation state (Eq. (2)) as those used to construct previous figures.

crystals. Since 1958, growth inhibition by absorbed impurities on crystal surfaces has been mainly described, and in some cases quantified, by the Cabrera–Vermilyea model. Although this model was originally proposed only for the inhibition of growth of crystals with fixed compositions, it can be generalised for the case of solid solutions. The generalisation presented in this paper reformulates the equations proposed by Cabrera and Vermilyea by introducing concepts from the theory of SS–AS systems. The new model provides a complete and consistent physical description of the inhibition behaviour of solid solution crystal surfaces by non-incorporating impurities. In the model, the critical supersaturation for complete inhibition is not a single number but a function of the solid solution composition. In addition, step kinetics above the critical supersaturation strongly depends on the supersaturation, which is also a function of the solid composition. As a consequence, an increase in the impurity concentration does not only affect the growth kinetics but also leads to changes in the composition of the steps. In this paper, the $Ba_xSr_{1-x}SO_4$–H_2O SS–AS system and a hypothetical non-incorporating impurity have been used for illustrative purposes. This SS–AS system is also suitable to conduct nanoscale experiments of crystal growth inhibition. Previous works have reported atomic force microscopy observations of the propagation of $Ba_xSr_{1-x}SO_4$ solid solution monosteps on barite (001) surfaces [10,30]. Furthermore, it has been shown that some phosphonates are effective inhibitors of growth on barite (001) surfaces [17,18]. Therefore, future observations and measurements of motion of monosteps on $Ba_xSr_{1-x}SO_4$ (001) surfaces in the presence of a constant concentration of phosphonates, and for different supersaturation states (i.e. different supersaturation functions), could be used to test the proposed model.

Acknowledgements

The author thanks Elena Pina for her critical reading of an earlier version of the manuscript. The paper benefited from thoughtful comments of two anonymous reviewers.

References

[1] N. Cabrera, D.A. Vermilyea, The Growth of Crystal from Solution, in: R.H. Doremus, B.W. Roberts, D. Turnbull (Eds.), Growth and Perfection of Crystals, Chapman & Hall, London, 1958, p. 393.
[2] M.L. Weaver, S.R. Qiu, J.R. Hoyer, W.H. Casey, G.H. Nancollas, J.J. De Yoreo, Chem Phys Chem 7 (2006) 2081.
[3] M.L. Weaver, S.R. Qiu, J.R. Hoyer, W.H. Casey, G.H. Nancollas, J.J. De Yoreo, Journal of Crystal Growth 306 (2007) 135.
[4] S. Mann, Biomineralization. Oxford, 2001.
[5] A. Putnis, C.V. Putnis, J.M. Paul, Proc. SPE Int. Symp. Oilfield Chemistry Paper SPE02094, 1995, p. 773.
[6] D. Bosbach, C. Hall, A. Putnis, Chemical Geology 151 (1998) 143.
[7] P. Risthaus, D. Bosbach, U. Becker, A. Putnis, Colloids and Surfaces A, Physiochemical and Engineering Aspects 191 (2001) 201.
[8] L. Legrand, P. Leroy, Prevention of Corrosion and Scaling in Water Supply Systems, Ellis Horwood, New York, 1990.
[9] J. Glater, in: K.S. Spiegler, A.D.K. Laird (Eds.), Principles of Desalination, academia Press, New York, 1980.
[10] C.M. Pina, M. Enders, A. Putnis, Chemical Geology 168 (2000) 195.
[11] M. Prieto, Thermodynamics of solid solution–aqueous solution systems, Reviews in Mineralogy and Geochemistry, MSA 70 (2009) 47.
[12] C.M. Pina, G. Jordan, in: G.Jordan, F. Brenker (Eds.), Reactivity of Mineral Surfaces at Nano-scale: Kinetics and Mechanisms of Growth and Dissolution, Nanoscopic Approaches in Earth and Planetary Sciences. EMU-notes, 8, 2010.
[13] S. Piana, F. Jones, J.D. Gale, Journal of the American Chemical Society 128 (2006) 13568.
[14] A. Stack, Journal of Physical Chemistry C 113 (6) (2009) 2104.
[15] S.N. Black, L.A. Bromley, D. Cottier, R.J. Davey, B. Dobbs, J.E. Rout, Journal Chemical Society Faraday Transactions 87 (1991) 3409.
[16] L.A. Bromley, D. Cottier, R.J. Davey, B. Dobbs, S. Smith, B.R. Heywood, Langmuir 9 (1993) 3594.
[17] F. Jones, W.R. Richmond, A. Rohl, The Journal of Physical Chemistry. B 110 (2006) 7414.
[18] C.M. Pina, C.V. Putnis, U. Becker, S. Biswas, E.C. Carroll, D. Bosbach, A. Putnis, Surface Science 553 (2004) 61.
[19] C.M. Pina, U. Becker, P. Risthaus, D. Bosbach, A. Putnis, Nature 395 (1998) 483.
[20] H.H. Teng, P.M. Dove, C.A. Orme, J.J. De Yoreo, Science 282 (1998) 724.
[21] M. Prieto, A. Putnis, L. Fernández-Díaz, Geological Magazine 130 (1993) 289.
[22] J.M. Astilleros, C.M. Pina, L. Fernández-Díaz, A. Putnis, Geochimica et Cosmochimica Acta 67 (2003) 1601.
[23] W.K. Burton, N. Cabrera, F.C. Frank, Philosophical Transactions of the Royal Society 243 (1951) 299.
[24] M. Ohara, P.C. Reid, Modelling Crystal Growth Rates from Solution, Prentice Hall, Inc, Englewood Cliffs, New Jersey, 1973, p. 272.
[25] T.A. Land, T.L. Martin, S. Potapenko, G.T. Palmore, J.J. De Yoreo, Nature399 (1999) 442.
[26] N. Kubota, Crystal Research and Technology 36 (2001) 8.
[27] P.M. Martins, A. Ferreira, S. Polanco, F. Rocha, A.M. Damas, P. Rein, Journal of Crystal Growth 311 (2009) 3841.
[28] J. Paquette, R. Reader, Geology 18 (1990) 1244.
[29] J. Rakovan, R. Reader, American Mineralogist 79 (1994) 892.
[30] C. YuHang, A. Asenjo, N. Sánchez-Pastor, L. Fernández-Díaz, J. Gómez, C.M. Pina, Surface Science 601 (2007) 381.